Science Advances
AAAS

Supplementary Materials for

Evidence for a neuromuscular circuit involving hypothalamic interleukin-6 in the control of skeletal muscle metabolism

Carlos Kiyoshi Katashima *et al.*

Corresponding author: Eduardo Rochete Ropelle, eduardoropelle@gmail.com

Sci. Adv. **8**, eabm7355 (2022)
DOI: 10.1126/sciadv.abm7355

The PDF file includes:

Other Supplementary Material for this manuscript includes the following:

Supplementary Materials

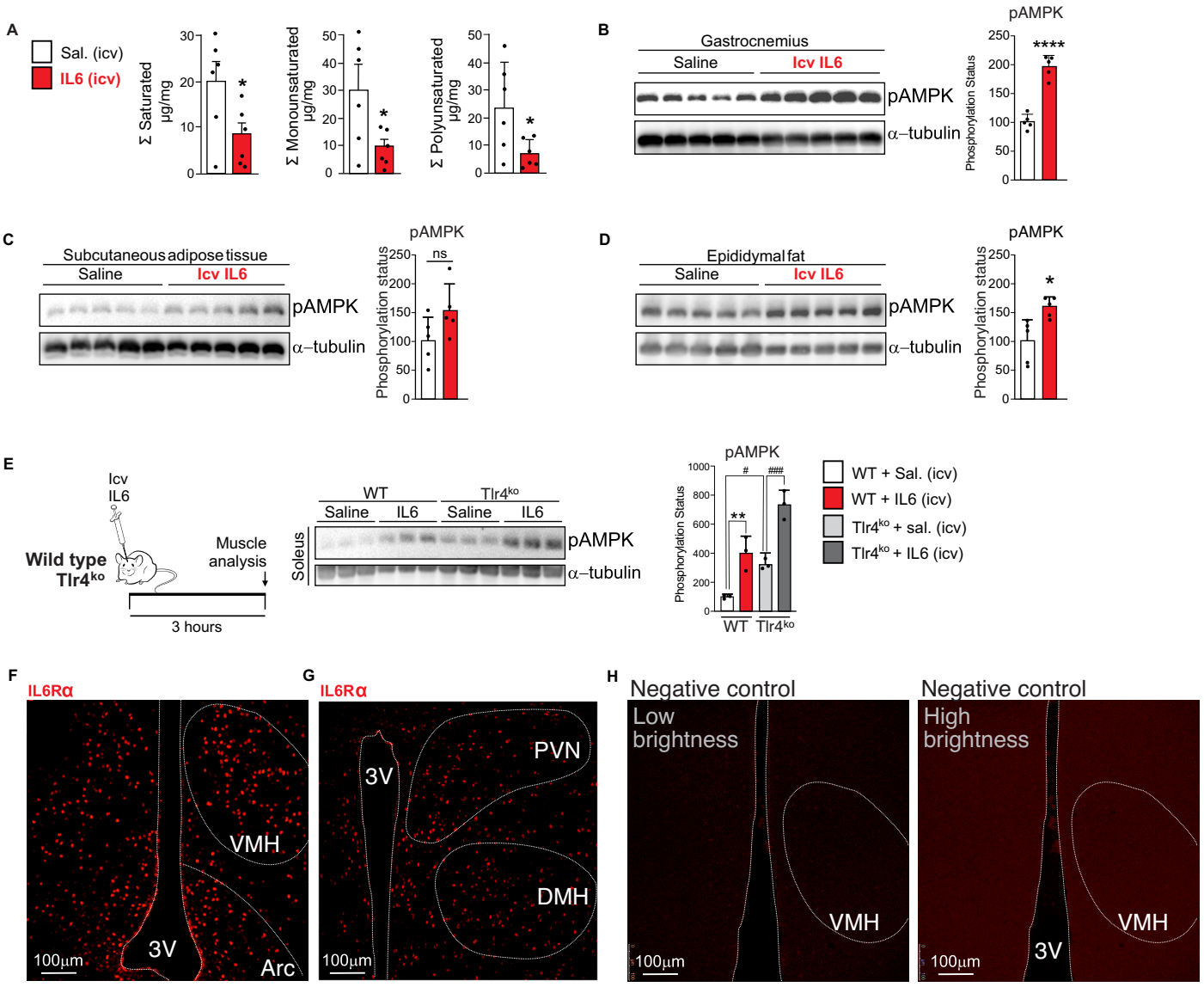

Figure S1. Effects of IL6 recombinant injection in peripheral metabolism and IL6R localization in hypothalamic tissue. (A) Determination of fatty acid fractions using mass spectrometry analysis in the gastrocnemius muscle 3 h after recombinant IL6 icv microinjection (n=6). Unpaired *t*-test was performed. (*, $p<0.05$, *vs* saline). AMPK^{Thr172} phosphorylation in; (B) gastrocnemius muscle, (C) adipose tissue and (D) epididymal fat, 3 hours after IL6 intracerebroventricular injection (200ng) (n=5). Unpaired *t*-test was. (*, $p<0.05$, *vs* saline and ****, $p<0.0001$, *vs* saline). (E) Wild type and Tlr4 knockout mice were icv injected with Il6 (200ng) and soleus muscle was removed 3 hours later for Western blot analysis (n=3). ANOVA one-way analysis was performed. (**, $p<0.01$, *vs* saline, #, $p<0.05$, *vs* saline and ###, $p<0.001$, *vs* Tlr4ko plus salilne). Immunostaining was performed to evaluate the distribution of IL6 receptor (red) in (F) arcuate and ventromedial nuclei (G) paraventricular and dorsomedial nuclei. (H) Negative control to confirm the specificity of IL6R antibody. Scale bars 100 µm (n=4).

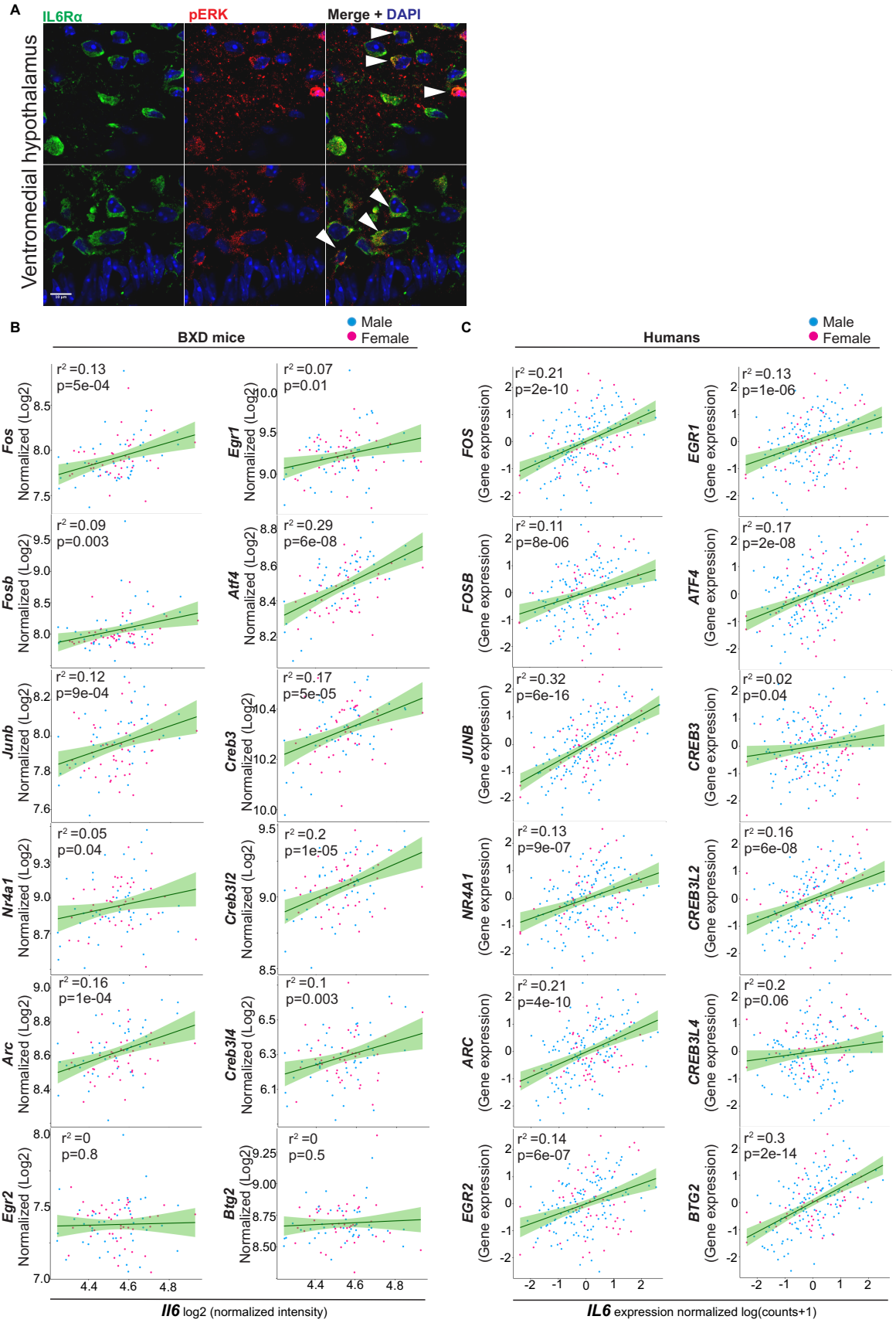

Figure S2. Association between IL6/ERK signaling and firing-rate related genes. (A) Confocal microscopy showing the co-localization of IL6 receptor (green) and pERK1/2 (red) in VMH of mice. White arrows indicate the co-localization (n=5, scale bars 10 µm). **(B, C)** *Il6* gene expression correlates positively with a set of firing-rate-related genes in the hypothalamus, both in a dataset of 50 BXD mouse strains (89 samples) and in the Genotype-Tissue Expression (GTEx) dataset of 170 deceased humans. The dark green lines show the best fit for linear relationships between the $\log_2$-transformed normalized expressions for each outcome gene and *Il6* (panel B) and between the GTEx normalized log-transformed gene expressions for each outcome gene and *IL6* (panel C). The corresponding 95% confidence bands are shown in light green. r^2 denotes the coefficient of determination, the proportion of the variation in the preprocessed outcome gene expressions that can be explained by the preprocessed gene expression of *Il6* (panel B) or *IL6* (panel C). *q* denotes the Benjamini-Hochberg false discovery rate-adjusted *p*-values. Males are shown in blue, females in pink.

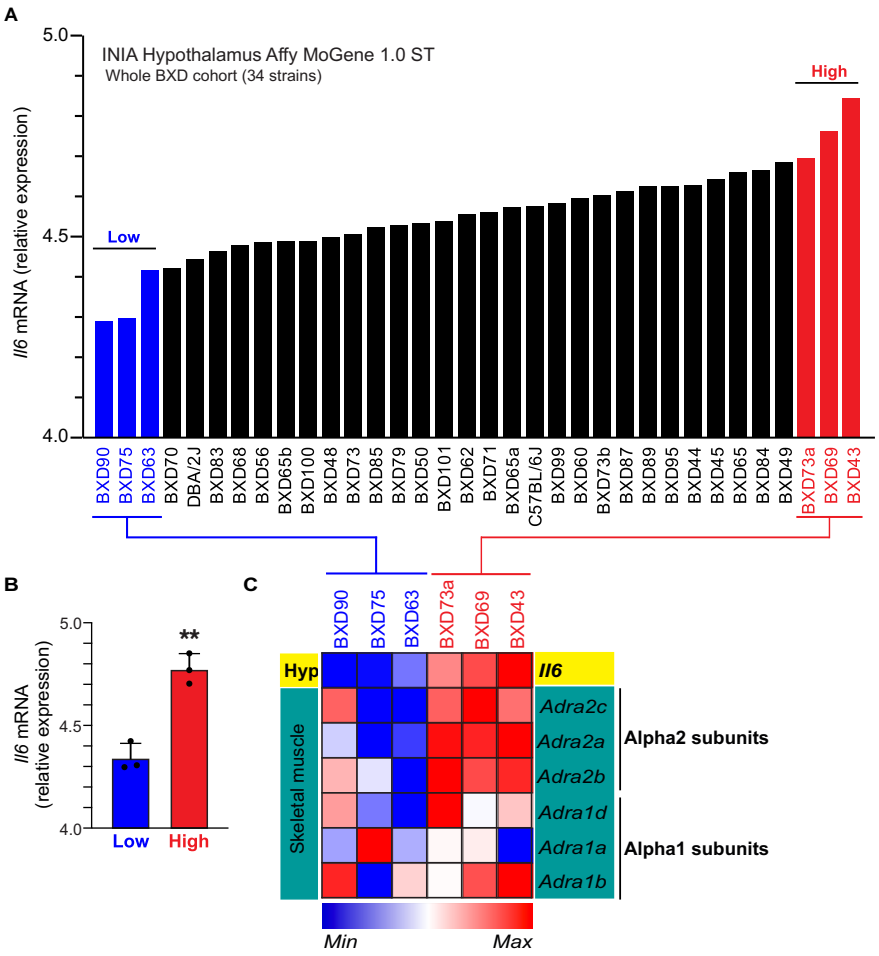

Figure S3. Evaluation of a-adrenergic receptors in BXD in mice. (A) Distribution of hypothalamic *Il6* gene expression in BXD cohort (34 strains). (B) Families containing the lowest (blue) and highest (red) in terms of hypothalamic *Il6* gene expression were studied. *t*-test was performed, $^{**}p<0.01$ *vs* Low group). Heat map graph using hypothalamic and muscle transcripts from Low and High groups.

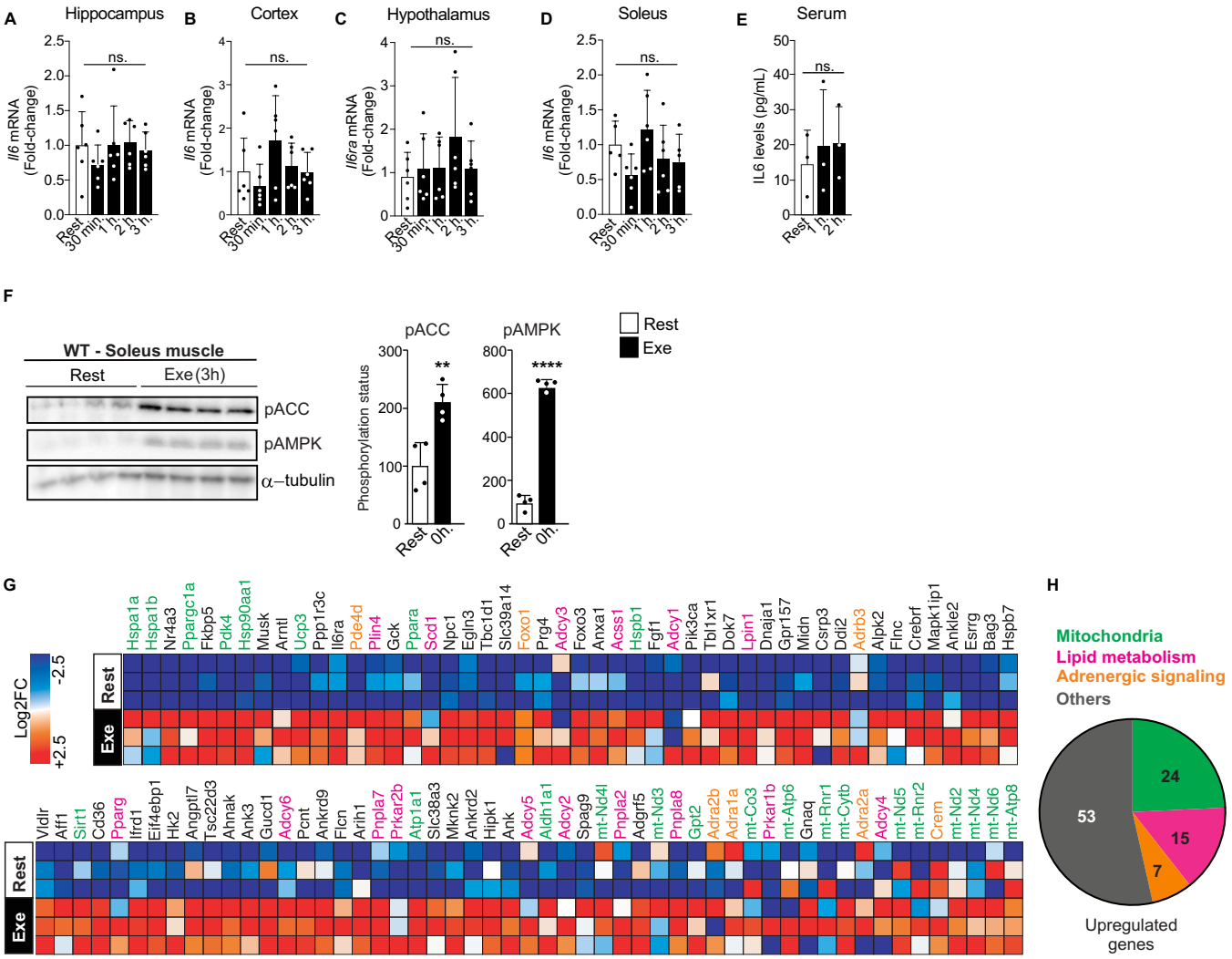

Figure S4. Evaluation of hypothalamus and skeletal muscle after acute exercise. *Il6* mRNA in; (A) hippocampus (n=6) and (B) cortex (n=6). (C) *Il6ra* mRNA in hypothalamus (n=6). *Il6* mRNA in; (D) soleus muscle (n=5-6). (E) IL6 serum levels (n=3). (F) ACC$^{Ser79/Ser212}$ and AMPK^{Thr172} phosphorylation in the soleus muscle 3 hours after the acute exercise. (G) RNAseq assay was performed using samples obtained 3 hours after the exercise protocol (n=3). (H) Up regulates genes showed in the heat map graph. One-way analysis of variance was used for statistical analysis in A-E. Unpaired *t*-test was used in F. (*, $p<0.05$, **, $p<0.01$ and ****, $p<0.0001$, *vs* rest). Non significant (ns).

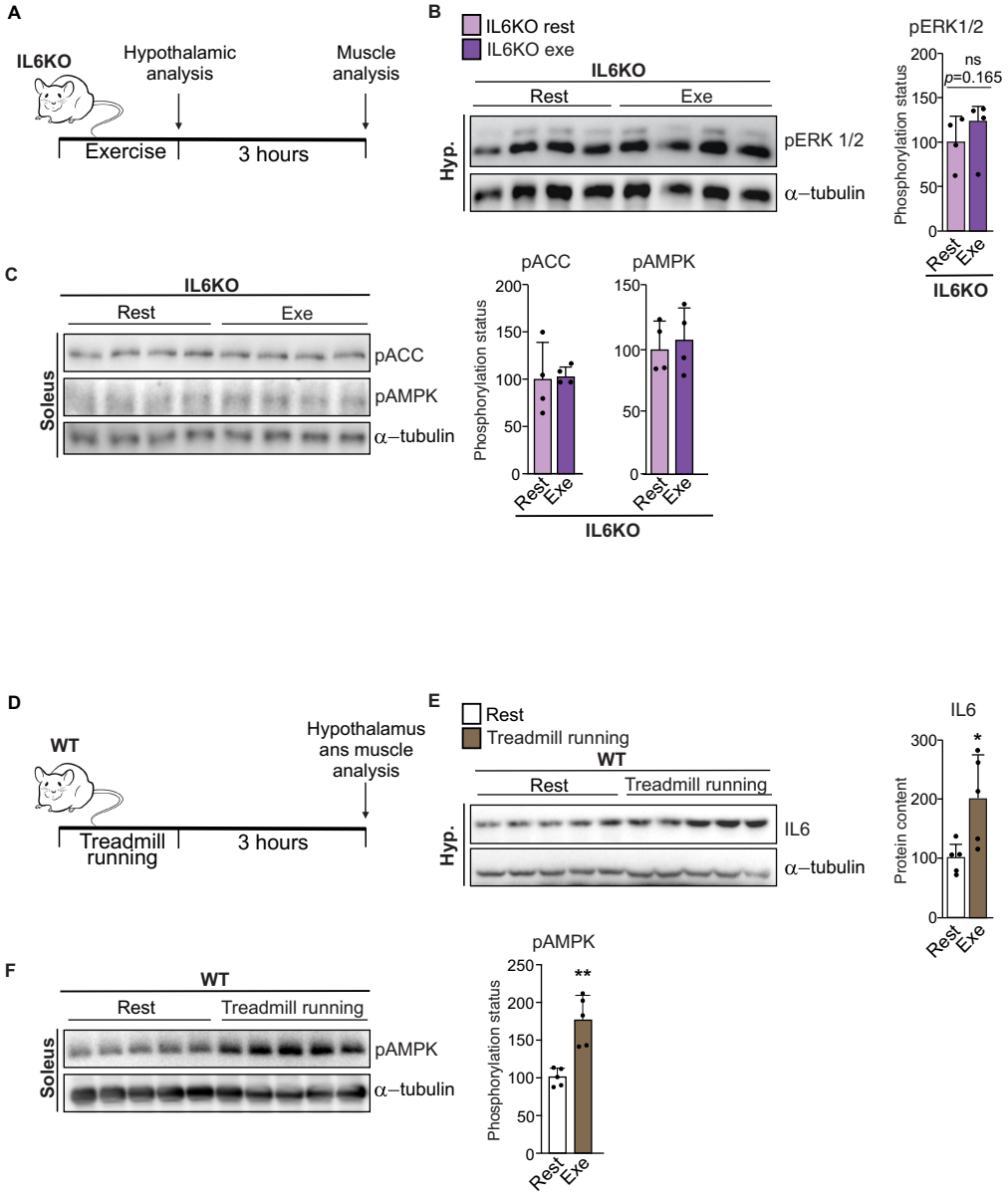

Figure S5. Evaluation of hypothalamus and skeletal muscle in response to acute exercise. (A) Experimental design involving IL6-null mice (IL6KO). (B) Hypothalamic ERK1/2 phosphorylation immediately after acute exercise (n=4) (C) $ACC^{Ser79/Ser212}$ and $AMPK^{Thr172}$ phosphorylation in soleus muscle 3 h after the exercise protocol (n=4). *t*-test was performed, ns, non-significative). (D) Experimental design involving acute treadmill running in wild type. (E) Hypothalamic IL6 protein content 3 h after the exercise (n=5) (F) $AMPK^{Thr172}$ phosphorylation in soleus muscle 3 h after the treadmill running protocol (n=5). *t*-test was performed. (*, $p<0.05$, *vs* Rest and (**, $p<0.01$, *vs* Rest).

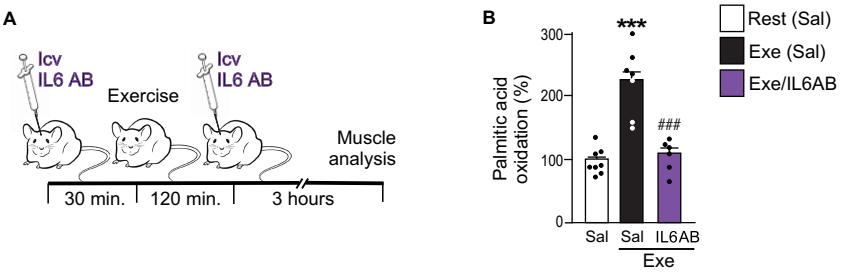

Figure S6. Effect of anti-IL6 antibody microinjection on fatty acid oxidation in muscle in exercised mice. (A) Experimental design. Microinjections of anti-IL6 antibody (100ng), were performed 30 minutes and immediately after the exercise protocol. The soleus muscle was removed 3 hours later. (B) Palmitic acid oxidation (n=6-8, ***, $p<0.001$ *vs* saline and $^{###}$, $p<0.001$ *vs* exercise+saline). One-way analysis of variance was performed.

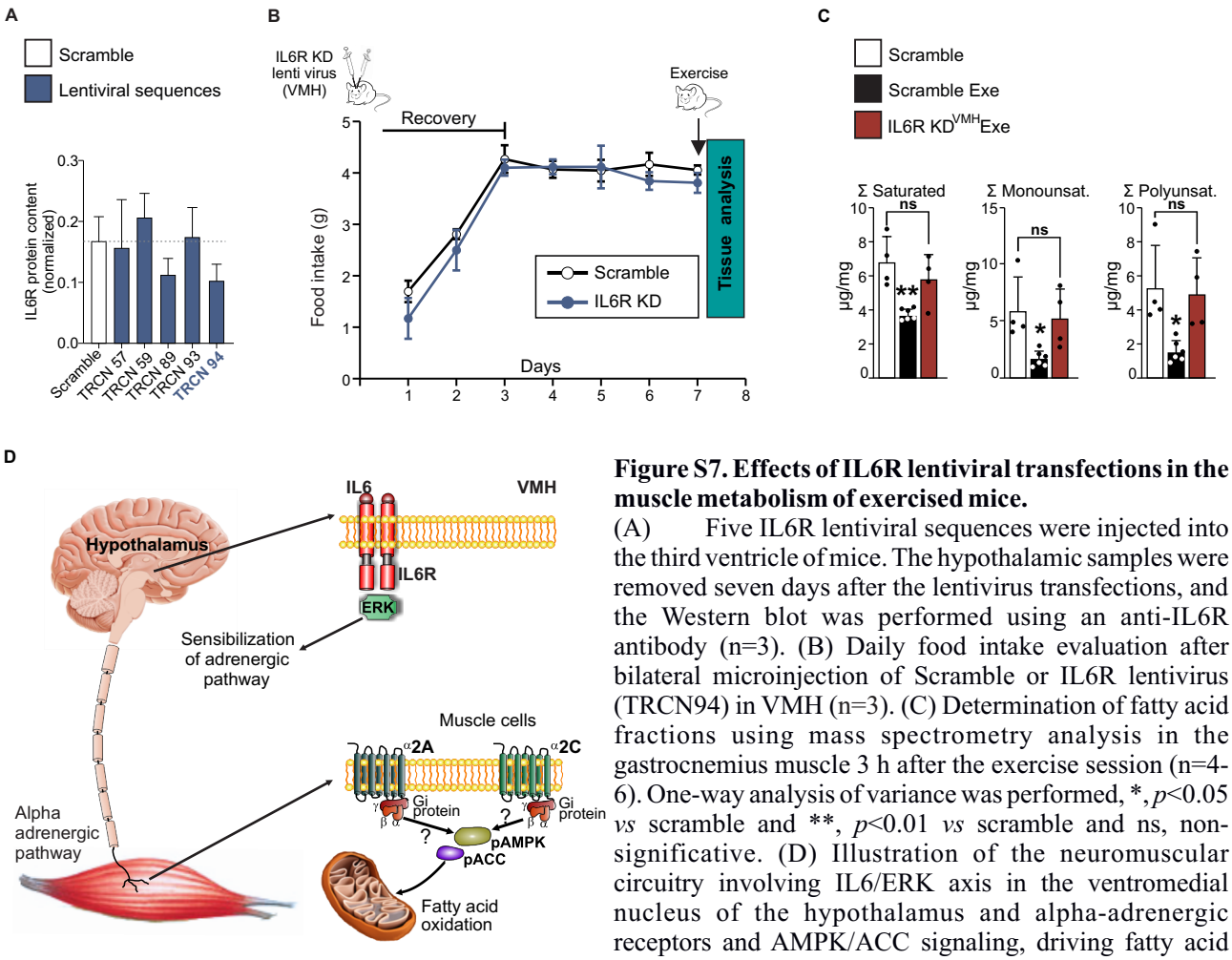

Figure S7. Effects of IL6R lentiviral transfections in the muscle metabolism of exercised mice.

(A) Five IL6R lentiviral sequences were injected into the third ventricle of mice. The hypothalamic samples were removed seven days after the lentivirus transfections, and the Western blot was performed using an anti-IL6R antibody (n=3). (B) Daily food intake evaluation after bilateral microinjection of Scramble or IL6R lentivirus (TRCN94) in VMH (n=3). (C) Determination of fatty acid fractions using mass spectrometry analysis in the gastrocnemius muscle 3 h after the exercise session (n=4-6). One-way analysis of variance was performed, *, $p<0.05$ *vs* scramble and **, $p<0.01$ *vs* scramble and ns, non-significative. (D) Illustration of the neuromuscular circuitry involving IL6/ERK axis in the ventromedial nucleus of the hypothalamus and alpha-adrenergic receptors and AMPK/ACC signaling, driving fatty acid oxidation in the skeletal muscle of mice.

Supplementary Material". This file contains data related to supplementary figures from S1 to S7.